JOURNAL OF GEOPHYSICAL RESEARCH, VOL. 102, NO. A4, PAGES 7179–7189, APRIL 1, 1997

Global structure of mirror modes in the magnetosheath

Jay R. Johnson and C. Z. Cheng

Princeton Plasma Physics Laboratory, Princeton University, Princeton, New Jersey

Abstract. A global stability analysis of mirror modes in the magnetosheath is presented. The analysis is based upon the kinetic-MHD formulation which includes relevant kinetic effects such as Landau resonance and gradient drift effects related to inhomogeneities in the background density, temperature, pressure and its anisotropy, magnetic field, and plasma flow velocity. Pressure anisotropy provides the free energy for the global mirror mode. The local theory of mirror modes predicts purely growing modes in the frame of the moving plasma confined to the unstable magnetosheath region; however, the nonlocal theory that includes the effects of gradients and plasma flow predicts modes with real frequency which propagate with the flow from the magnetosheath toward the magnetopause boundary. The real frequency is of the order of a combination of the diamagnetic drift frequency and the Doppler shift frequency associated with plasma flow. The real frequency is not simply a Doppler-shifted frequency obtained from local calculation. Rather, it is determined from a boundary value constraint on an eigenvalue problem and can differ significantly from the local Doppler-shifted frequency. Without plasma flow, the diamagnetic drift frequency provides a wave phase velocity in the direction of the magnetopause so that wave energy accumulates against the magnetopause boundary, and the amplitude is skewed in that direction. Such a wave structure might be observed under conditions of small magnetosheath flow. For larger plasma flow (Alfvén Mach number ≥ 0.1), the flow also causes a real phase velocity in the direction of the flow, but the phase velocity increases from a small value near the bow shock to nearly the flow velocity as the wave propagates toward the magnetopause. As a result, wave amplitude is large where the phase velocity is small and small where the phase velocity is large resulting in a skew in wave amplitude toward the bow shock.

Introduction

Identification of observed compressional waves in the magnetosheath has been somewhat controversial. Indeed, many observations have found low-frequency MHD waves with density and magnetic field out of phase. These waves have been interpreted as being either slow modes or mirror modes. *Gleaves and Southwood* [1991] observed compressional waves in the magnetosheath near the magnetopause and identified them as slow modes because those waves had a finite phase velocity toward the magnetopause in a different direction from the flow velocity. They dismissed those waves as being mirror modes based on the prediction of the uniform plasma theory that mirror modes are purely growing waves in the plasma rest frame so that they should be observed to propagate only with the flow direction in contrast to their observations. However, it is commonly believed that strong Landau damping of the slow mode in the magnetosheath inhibits its growth, and therefore observations of waves with antiphase correlation between density and magnetic field were identified as drift mirror modes [*Tsurutani et al.*, 1982; *Hubert et al.*, 1989; *Anderson et al.*, 1994; *Denton et al.*, 1995].

More recently, the work of *Song et al.* [1994] and *Denton et al.* [1995] addressed mode identification in the magnetosheath and near the magnetopause. The analysis of *Denton et al.* [1995] identified the bulk of the observed waves near the magnetopause to be mirror modes. On the other hand, *Song et al.* [1994] identified waves throughout the magnetosheath and found that while fast magnetosonic and mirror mode waves appear to be dominant in the middle magnetosheath, fast and slow magnetosonic waves are dominant near the magnetopause. In their argument based on uniform plasma theory the essential measurement that distinguishes between the mirror mode and slow magnetosonic waves is the so-called Doppler ratio, which is used to determine whether the wave has a finite phase velocity relative to the bulk plasma flow. Using two satellites they were able to determine that compressional waves observed just upstream of the magnetopause have antiphase relationship between magnetic field and density. Because they stand in the flow and therefore have a finite up-

Copyright 1997 by the American Geophysical Union.

Paper number 96JA03949.
0148-0227/97/96JA-03949$09.00

stream phase velocity in the frame of the flow, they were identified as slow modes.

The one-dimensional hybrid simulation of *Omidi and Winske* [1995] provides some insight as to a possible resolution of this controversy. In that simulation, a fast shock wave propagates away from a rotational discontinuity. Mirror mode waves arise in the wake of the shock due to pressure anisotropy and are carried against the rotational discontinuity by plasma flow. Near the region where the magnetic field increases, large amplitude waves appear to stand between the rotational discontinuity and the region of low plasma-β referred to as a magnetic boundary. The waves appeared to stand in the flow and had finite real frequency relative to the plasma flow. *Omidi and Winske* [1995] called the waves MIAOW (mirror and slow mode), although it appears that the waves are simply mirror modes that pile up at the magnetopause boundary. In the simulation the MIAOW waves were found to only occur for finite normal magnetic field. Indeed, as stated in our Local Theory section, the mirror mode exists only for $\omega < k_{\|} v_{thi}$, and if there were no normal magnetic field component, then $\mathbf{k} \cdot \mathbf{B} = 0$, $\omega > k_{\|} v_{thi}$, and there is no instability.

In this paper, we present an analysis of global mirror modes at the magnetopause based upon the kinetic-MHD approach which is an attempt to incorporate the most important ion kinetic effects into the MHD formalism [*Cheng*, 1991; *Cheng and Johnson*, 1996]. The gyrokinetic equation, which is essentially the gyroaveraged Vlasov equation, is the cornerstone of the kinetic part of the model for this application. Moments of the gyrokinetic equation are taken and provide a modified momentum equation and Ohm's law. This approach retains the important kinetic effects of Landau damping and diamagnetic drift as well as the physics associated with the ion magnetic gradient and curvature drifts. We shall show that it is important to retain both these kinetic effects and global effects associated with gradients in the background profiles of density, temperature and magnetic field. The results we obtain are in qualitative agreement with many properties of compressional waves observed in the magnetosheath.

The mirror modes destabilized in the magnetosheath are of substantial interest because they can couple a significant amount of wave energy from the magnetosheath to waves at the magnetopause. Local mirror mode theory predicts that the mirror mode is purely growing in the frame moving with the plasma. In this work we shall study the nonlocal effects of realistic background gradients and plasma flow in a frame in which the bow shock and magnetopause are stationary and determine that the eigenfrequency is complex with a substantial real component due to particle diamagnetic drift and Doppler shift associated with plasma flow. The real frequency, however, is different from the local Doppler shift and therefore corresponds to a wave structure that moves relative to the plasma flow. Because these waves have a real frequency they can couple to kinetic Alfvén waves near the magnetopause where this frequency is close to the Alfvén resonance frequency. Mode converted kinetic Alfvén waves may play an important role in transport processes at the magnetopause [*Hasegawa and Mima*, 1978; *Lee et al.*, 1994; *Johnson and Cheng*, 1995].

The organization of this paper is as follows. We shall briefly review the mirror mode and point out the important consequences introduced by (1) background gradients in the equilibrium and (2) kinetic effects. We present the kinetic-MHD model for the mirror mode which includes these effects. Then, we solve for the global mirror eigenmodes using a one-dimensional equilibrium based upon typical observations and interpret the results. Then we present a discussion of our results in relation to wave observations and simulation results. Finally, we give a summary.

Background Gradient and Kinetic Effects on Mirror Modes

Without kinetic effects, low-frequency ($\omega \ll k_{\|} v_A$, $k_{\|} c_s$, where $k_{\|}$ is the parallel wave number, v_A is the Alfvén speed, and c_s is the sound speed) compressional magnetic field fluctuations in a plasma with flow velocity $\mathbf{V}_0$ may be described by the MHD equations. With appropriate projections of the momentum equation, it is possible to isolate the predominantly compressional mode [*Cheng*, 1991, see equations (21) and (65)].

$$\frac{\rho}{B^2}\left(\frac{\partial}{\partial t} + \mathbf{V}_0 \cdot \nabla\right)^2 \mathbf{B} \cdot \delta\mathbf{B} = \mathbf{B} \cdot \nabla\left(\frac{\sigma}{B^2}\mathbf{B} \cdot \nabla\mathbf{B} \cdot \delta\mathbf{B}\right) + \nabla_{\perp}^2 \left(\tau_{MHD}\mathbf{B} \cdot \delta\mathbf{B}\right) \quad (1)$$

where the firehose and mirror instability parameters are

$$\sigma = 1 + (\beta_{\perp} - \beta_{\|})/2 \quad (2)$$

$$\tau_{MHD} = 1 + \beta_{\perp}(1 - \beta_{\perp}/\beta_{\|}), \quad (3)$$

respectively, for bi-Maxwellian plasmas. The uniform plasma dispersion relation for waves without background flow is $\omega^2 = \sigma k_{\|}^2 v_A^2 + \tau_{MHD} k_{\perp}^2 v_A^2$ which reduces in the isotropic limit ($\sigma = \tau = 1$) to the well-known compressional Alfvén wave. In a plasma with $\beta_{\perp} > \beta_{\|} \sim 1$, $\tau_{MHD} < 0$ can lead to the well-known purely growing mirror instability.

Mirror modes are unstable and can grow to large amplitudes because the magnetosheath is characterized by a large pressure anisotropy [*Anderson et al.*, 1991; *Paschmann et al.*, 1993]. Pressure anisotropy develops in the magnetosheath because as plasma crosses the bow shock, the magnetic field increases and the flow velocity perpendicular to the magnetic field is converted into gyromotion yielding a large perpendicular plasma temperature. Motion along the magnetic field is not readily converted into thermal energy so that a large anisotropy develops with $\beta_{\perp} > \beta_{\|}$. In the

magnetosheath the kinetic pressure dominates the relatively weak magnetic field so that typically $\beta > 1$. For $\beta_\perp/\beta_\parallel > (1 + 1/\beta_\perp)$ the plasma is unstable to the well-known mirror mode, and *Phan et al.* [1996] have shown that low-frequency compressional wave activity has a strong dependence on this condition in the magnetosheath. Toward the magnetopause, the flow slows down and the magnetic field further increases while the plasma pressure decreases and becomes more isotropic. The plasma β falls to a more typical magnetospheric value much less than 1 which suppresses the mirror mode instability.

Modifications to the simplistic uniform plasma MHD description of the compressional wave can be significant. In the magnetosheath and near the magnetopause it is important to consider the effects of gradients in the equilibrium as well as kinetic effects. The parameter τ_{MHD}, which indicates regions of local instability when negative, has a profile which changes from positive in the solar wind (relatively isotropic pressure) to negative in the magnetosheath (due to large pressure anisotropy) to positive in the magnetosphere (low β, less anisotropy). As a consequence, (1) describes a purely growing eigenmode localized in the region of instability. The usefulness of local theory based upon homogeneous plasma is somewhat questionable for this situation because the frequencies are determined as a global property and the spatial behavior of the mode can vary substantially over the domain of interest.

A second source of modification to uniform plasma theory results because the plasma flows relative to somewhat stationary boundaries (the bow shock and magnetopause). In an infinite plasma with uniform plasma flow an observer at a stationary point relative to the moving plasma would observe the frequency in the plasma frame Doppler shifted by a real frequency. However, because the structure is somewhat tied to the boundaries through boundary conditions, the Doppler shift tends not to be a constant even if the flow is uniform. As a result, the global real frequency is an average value of the Doppler shift. Furthermore, if the background plasma flow is nonuniform, the Doppler shift varies over the entire spatial domain and again the global real frequency turns out to be an average Doppler shift. Hence the effects of nonuniform plasma flow turn out to be important in both the MHD and kinetic parts of the kinetic-MHD equations, and the solutions that we obtain have substantially different character when plasma flow is increased.

MHD wave analysis effectively deals with complicated boundary conditions and global gradients but fails to account for important kinetic effects. *Hasegawa* [1969] first provided a description of kinetic effects on the mirror mode. Moreover, an armada of studies of kinetic effects on mirror modes in the magnetosheath has been amassed using Vlasov theory based upon a homogeneous background [*Gary*, 1992; *Gary et al.*, 1993a,b,c; *Gary and Winske*, 1993; *Denton et al.*, 1995]. While these calculations provide very useful information about local threshold conditions, they do not account for kinetic effects that involve background gradients and boundary conditions. On the other hand, MHD wave analysis effectively deals with complicated boundary conditions and global gradients but fails to account for important kinetic effects.

If kinetic effects are included in (1), kinetic contributions arise which modify the term proportional to τ_{MHD} so that τ_{MHD} must be replaced by an appropriate kinetic τ which contains effects of diamagnetic drift, wave-particle resonances, and finite Larmor radii. In the low-frequency limit ($\omega \ll k_\parallel v_{th\parallel}$), the kinetic τ reduces to τ_{MHD}. It has already been shown that kinetic effects strongly affect the MHD picture of the mirror instability. If ($\omega \sim k_\parallel v_{th\parallel}$), then wave particle resonance is important. *Southwood and Kivelson* [1993] provided an excellent physical picture of the kinetic effects on the instability and relates the instability to resonant particles with zero phase velocity. An important feature of the kinetic dispersion relation is that for an anisotropic plasma, in addition to the weakly damped fast magnetosonic wave found in the limit $\omega \gg k_\parallel v_{th\parallel}$, the mirror mode is found with $\omega \ll k_\parallel v_{th\parallel}$. For low frequencies ($\omega \ll k_\parallel v_{th\parallel}$), the kinetic mirror mode is reasonably approximated by the MHD description for the threshold condition. However, when $\omega \sim k_\parallel v_{th\parallel}$, the kinetic mirror mode growth rates are significantly reduced from the prediction of MHD theory.

Other kinetic effects not described by uniform plasma Vlasov theory also arise where pressure and density gradients are important. The gradients enter into the kinetic description through the diamagnetic drift. These effects were first described as the drift-mirror mode [*Hasegawa*, 1969] but were thought to be unimportant because pressure and density gradients in the magnetosheath are generally small; however, we shall show that large localized gradients at the magnetopause can affect the global structure and provide a real frequency to the mirror mode. At the magnetopause, the diamagnetic drift frequency, $\omega_* \sim k_\perp v_{thi}\rho_i/L_{MP}$ (L_{MP} is the gradient scale at the magnetopause and ρ_i is the ion gyroradius) can be significant because, for typical magnetopause parameters, $\omega_* \sim k_\parallel v_{thi}$ and wave-particle interaction is strongly modified.

Kinetic-MHD Eigenmode Equation for Mirror Modes

An appropriate description of the mirror mode in the magnetosheath and near the magnetopause should attempt to account for the effects outlined in the last section. In particular, the model should contain the global profile effects which arise from inhomogeneous flow velocity, density, pressure, temperature, and magnetic field. Moreover, the model should contain important kinetic effects associated with the wave-particle inter-

action and diamagnetic drift. The kinetic-MHD model, which retains all of these effects is appropriate because the smallest background scale (the magnetopause) is typically the order of 10 ρ_i and thus satisfies the gyrokinetic approximation. The gyrokinetic formalism allows us to solve the gyroperiod averaged Vlasov equation. The intrinsic assumptions involved are that $\omega \ll \Omega_i$ (the ion gyrofrequency), $\rho_i \ll L_\perp, L_\parallel$ where $L_\perp$ and $L_\parallel$ are gradient scale lengths parallel and perpendicular to the magnetic field. The wave field may have variation of the order of the gyroradius so that $k_\perp \rho_i \sim 1$ is allowed and $k_\perp \gg k_\parallel$. Finally, $k_\parallel L_\parallel \gg 1$ and $k_\perp L_\perp \gg 1$, but we point out that $k_\parallel L_\perp \sim 1$ is allowed. All of these conditions are generally met at the magnetopause for these waves. To focus on the effects described above, we take for simplicity a one-dimensional equilibrium in the x direction which is taken to be normal to the magnetopause.

As a first test of the importance of gyrokinetic effects and global structure on magnetosheath mirror waves, it is reasonable to consider solutions based upon a one-dimensional equilibrium. Although the results can be expected to be significantly different in two or three dimensions, we a primarily interested in assessing the importance of kinetic and nonlocal effects relative to the results of local theory, for which one-dimensional calculations should suffice. We should point out that it should be straightforward to generalize this model to account for realistic two- or three-dimensional equilibrium profiles. All equilibrium quantities will be functions of x only. For simplicity, we take the magnetic field and velocity to be $B_0(x)\hat{z}$ and $V_0(x)\hat{x}$, respectively. We neglect drifts due to magnetic field gradients and curvature in the resonant wave-particle interaction which should not be important because $k_\parallel v_{th}$ is relatively large compared with the drift terms $\mathbf{k}\cdot\mathbf{v}_d$. Coupling to transverse magnetic fluctuations is ignored. It is usually the case that coupling is significant near the Alfvén and sound resonances where $\omega = k_\parallel v_A$ and $\omega = k_\parallel c_s$ respectively [e.g., *Chen and Hasegawa*, 1974]; however, the waves that we consider have low frequency: $\omega < k_\parallel c_s$ and $\omega < k_\parallel v_A$ so that coupling is small throughout most of the domain. Obviously, if the magnetic field were to rotate so that $\mathbf{k}\cdot\mathbf{B} = 0$ such coupling would be very important. We do expect that there will be localized coupling where the wave phase velocity approaches v_A or c_s leading to mode conversion to kinetic Alfvén waves or damping from the sound continuum. Also, we refer the reader to the Discussion of Results section where we discuss the importance of coupling to the slow wave near the location $\tau = M_A^2$.

The global kinetic-MHD equation describing the compressional magnetic field is given by [*Cheng*, 1991]

$$\frac{\rho}{B^2}\left(\frac{\partial}{\partial t} + \mathbf{V}_0\cdot\nabla\right)^2 \mathbf{B}\cdot\delta\mathbf{B} = \mathbf{B}\cdot\nabla\left(\frac{\sigma}{B^2}\mathbf{B}\cdot\nabla\mathbf{B}\cdot\delta\mathbf{B}\right) + \nabla_\perp^2\left(\tau\mathbf{B}\cdot\delta\mathbf{B}\right) \quad (4)$$

with

$$\tau\mathbf{B}\cdot\delta\mathbf{B} \equiv \tau_{MHD}\mathbf{B}\cdot\delta\mathbf{B} + \delta\hat{p}_\perp, \quad (5)$$

and the nonadiabatic pressure response $\delta\hat{p}$ is

$$\delta\hat{p}_\perp = m\int d^3v(\mathbf{v}_\perp - \mathbf{V_0})^2 g/2. \quad (6)$$

The nonadiabatic particle distribution g evolves according to the gyrokinetic equation which is given by

$$(\omega + i\mathbf{v}_\parallel\cdot\nabla + i\mathbf{V_0}\cdot\nabla)g = -\frac{q}{m}\frac{\partial F}{\partial\mathcal{E}}(\omega-\omega_*)\frac{\omega v_\perp}{k_\perp}J_1(k_\perp v_\perp/\Omega)\frac{\mathbf{B}\cdot\delta\mathbf{B}}{B}, \quad (7)$$

where $\mathcal{E} = v^2/2$, Ω is the cyclotron frequency, and $\omega_* = \mathbf{B}\times\mathbf{k}_\perp\cdot\nabla F/(B\Omega\partial F/\partial\mathcal{E})$. It is implicitly understood that ω, $k_\perp$, and ω_* (through $\mathbf{k}_\perp$) are formal operators corresponding to $\omega \to i\partial/\partial t$ and $\mathbf{k}_\perp \to -i\nabla_\perp$ [*Frieman and Chen*, 1982]. In (7) we have dropped terms related to electrostatic potential as well as magnetic gradient and curvature drifts. In deriving (4) we have also dropped terms which couple to the transverse magnetic field through the pressure gradient and magnetic field curvature. However, (4) contains the essential kinetic effects required to replicate the well-known drift mirror mode dispersion relation [*Hasegawa*, 1969]. If we assume $k_\perp\rho_i < 1$, we may expand the Bessel function to retain nonlocal effects in (7). Formally, if the wave field varies more rapidly than the background plasma we may replace $\mathbf{V}_0\cdot\nabla g$ by $g\mathbf{V}_0\cdot\nabla\delta B_\parallel/\delta B_\parallel$ in (7). This approximation is equivalent to a WKB approximation in the $\hat{\mathbf{x}}$ direction. Corrections due to this approximate proceedure are $\mathcal{O}(\lambda/L)$, where λ is the wavelength of the wave field and L is the background gradients scale. This is a reasonable approximation except perhaps at the magnetopause boundary. We verify the validity of that approximation a posteriori by comparing the local $\mathbf{k}_\perp$ with the gradient scale length. From (6) we obtain

$$\delta\hat{p} = -\frac{\beta_\perp T_\perp}{T_\parallel}\Big[(\zeta-\zeta_*^{(1)})Z(\zeta)2\mathcal{I}_3/\lambda - \zeta_*^{(2)}Z(\zeta)2\mathcal{I}_5/\lambda - \zeta_*^{(3)}\zeta(1+\zeta Z(\zeta))2\mathcal{I}_3/\lambda\Big]\mathbf{B}\cdot\delta\mathbf{B} \quad (8)$$

$$\zeta = \frac{(\omega - iV_0\cdot\nabla)}{\sqrt{2}k_\parallel v_{th\parallel}} \quad (9)$$

$$\zeta_*^{(1)} = \frac{\mathbf{b}\times\mathbf{k}_\perp v_{th\perp}}{\sqrt{2}k_\parallel v_{th\parallel}}\rho_i\left(\frac{\nabla n}{n} - \frac{1}{2}\frac{\nabla T_\parallel}{T_\parallel} - \frac{\nabla T_\perp}{T_\perp}\right) \quad (10)$$

$$\zeta_*^{(2)} = \frac{\mathbf{b}\times\mathbf{k}_\perp v_{th\perp}}{\sqrt{2}k_\parallel v_{th\parallel}}\rho_i\left(\frac{\nabla T_\perp}{T_\perp}\right) \quad (11)$$

$$\zeta_*^{(3)} = \frac{\mathbf{b}\times\mathbf{k}_\perp v_{th\parallel}}{\sqrt{2}k_\parallel v_{th\parallel}}\rho_i\left(\frac{\nabla T_\parallel}{T_\parallel}\right) \quad (12)$$

where $\lambda = k_\perp^2\rho_i^2/2$. The integral operators, $\mathcal{I}_3, \mathcal{I}_5$ are defined in the appendix and involve integrals over

Bessel's functions. For small $k_\perp \rho_i$, $2\mathcal{I}_3/\lambda \sim 1$ and $2\mathcal{I}_5/\lambda \sim 3$.

Boundary conditions at the bow shock and magnetopause are critical in determining the structure of the modes. Because the group velocity of the modes that we consider is far less than the flow velocity in the solar wind, no wave information can be carried upstream across the bow shock. This property is manifest in a singularity at the location where $\tau_{MHD} = (V_0/v_A)^2 = M_A^2$. At that location, the group velocity of compressional waves propagating against the flow approaches zero. A careful expansion of the MHD equations near this point indicates that the solution can consist of two Frobenius solutions, one of which is a power series and the other dominated by a logarithmic singularity. The behavior of the solutions is very similar to the behavior of MHD solutions near the well-known field line resonance [*Chen and Hasegawa*, 1974]. In this case, however, we choose the coefficient of the logarithmic solution to vanish because there is no physical mechanism which can provide the buildup of energy at the boundary. The remaining solution behaves like $c(1+\eta^2 x + ...)$, where $\eta = \omega/\nabla V_0$ with $\eta \ll 1$ for a sharp boundary. In essence, this means that $d\delta B_\parallel/dx \approx 0$ near the boundary which can be interpreted as a reflecting boundary condition. The amplitude of the wave should reduce to zero in a small boundary layer near the bow shock when appropriate kinetic effects and coupling are included. We take the approximation $d\delta B_\parallel/dx \approx \eta^2$ near the bow shock in all of our results. On the magnetospheric side of the magnetopause we take the boundary condition that the solution connects to the appropriate exponentially decaying Eikonal solution which we obtain implicitly from the differential equation.

Local Theory

To get a better understanding of the physical meaning of the kinetic-MHD eigenmode equation, we can investigate local theory with a WKB representation, $\delta B_\parallel = \delta \bar{B} e^{i(\mathbf{k}\cdot\mathbf{x}-\omega t)}$ for which $\nabla \to i\mathbf{k} = i\mathbf{k}_\perp + ik_\parallel \mathbf{b}$. We also assume small $k_\perp \rho_i$. The local dispersion relation obtained from (4), (5), and (8)-(12) becomes

$$(\omega - \mathbf{k}\cdot\mathbf{V}_0)^2 = \sigma k_\parallel^2 v_A^2 + \tau k_\perp^2 v_A^2 \tag{13}$$

where

$$\tau = 1 + \beta_\perp \left\{1 - \beta_\perp/\beta_\parallel \left[1 + \left(\zeta - \zeta_*^{(1)}\right) Z(\zeta) 2\mathcal{I}_3/\lambda \right.\right.$$
$$\left.\left. -\zeta_*^{(2)} Z(\zeta) 2\mathcal{I}_5/\lambda - \zeta_*^{(3)} \zeta (1 + \zeta Z(\zeta)) 2\mathcal{I}_3/\lambda\right)\right]\right\} \tag{14}$$

From the appropriate limits it is not difficult to see that this dispersion relation governs propagation of compressional Alfvén (fast magnetosonic) waves for $(\omega - \mathbf{k}\cdot\mathbf{V}_0) > k_\parallel v_{thi}$ and the mirror mode for $(\omega - \mathbf{k}\cdot\mathbf{V}_0) < k_\parallel v_{thi}$. Without diamagnetic drift effects, the frequency and damping rate of the weakly damped magnetosonic wave are given by

$$\omega_r \approx \mathbf{k}\cdot\mathbf{V}_0 \pm [\sigma k_\parallel^2 + (1+\beta_\perp) k_\perp^2]^{1/2} v_A$$
$$\omega_i \approx -\sqrt{2\pi} k_\perp v_{th\parallel} \frac{\beta_\perp^2}{\beta_\parallel^2} \frac{k_\perp}{k_\parallel} \exp[-(\frac{\sigma}{\beta_\parallel} + \frac{(1+\beta_\perp)}{\beta_\parallel} \frac{k_\perp^2}{k_\parallel^2})] \tag{15}$$

Even in a high-β plasma the damping is relatively weak and is negligible for $k_\perp > k_\parallel$. The diamagnetic drift modifies the fast magnetosonic wave dispersion relation so that

$$(\omega - \mathbf{k}\cdot\mathbf{V}_0)^2 = \sigma k_\parallel^2 v_A^2 + (1 + \beta_\perp - \frac{\beta_\perp^2}{\beta_\parallel} \frac{\tilde{\omega}_*}{(\omega - \mathbf{k}\cdot\mathbf{V}_0)}) k_\perp^2 v_A^2 \tag{16}$$

(the Landau damping terms are exponentially small in this approximation) and the magnetosonic wave is coupled with a drift wave characterized by the frequency, $\tilde{\omega}_* = \sqrt{2} k_\parallel v_{th\parallel} (\zeta_*^{(1)} + 3\zeta_*^{(2)} + \zeta_*^{(3)}/2)$. If the drift frequency is small, coupling between the magnetosonic wave and the drift wave is small, and there is a slight modification in the real frequency of the mode.

Finally, it is useful to obtain the kinetic mirror mode dispersion relation in the low frequency limit. In this limit we take $((\omega - \mathbf{k}\cdot\mathbf{V}_0) < k_\parallel v_{thi}, \omega_* < k_\parallel v_{thi}$ and $(\omega/k_\perp v_A)^2 < \omega/k_\parallel v_{thi})$ in (13) and (14) to obtain

$$\omega = \mathbf{k}\cdot\mathbf{V}_0 + \hat{\omega}_* - ik_\parallel v_{th\parallel} \sqrt{\frac{2}{\pi}} \frac{T_\parallel}{\beta_\perp T_\perp} \left(\frac{\sigma k_\parallel^2}{k_\perp^2} + \tau_{MHD}\right) \tag{17}$$

where $\hat{\omega}_* = (3\omega_{*p} - \omega_{*n})/2$ with $\omega_{*n} = -\rho_i v_{th\perp} \mathbf{b} \times \mathbf{k}\cdot\nabla n/n$ and $\omega_{*p} = -\rho_i v_{th\perp} \mathbf{b} \times \mathbf{k}\cdot\nabla P/P$. The first two terms in the dispersion relation are real frequency modification due to Doppler shift and diamagnetic drift respectively. The last term is the linear growth rate for the mirror mode. Without plasma flow and temperature gradient, the dispersion relation reduces to the drift mirror mode given by *Hasegawa* [1969]. Notice that the stability criterion remains the same as for fluid theory; however, unlike fluid theory the growth rate scales with $k_\parallel$.

In (18) one can more readily see the effects of the Doppler shift and the diamagnetic drift in making a contribution to the real frequency of the mode. We can expect that the real frequency of the eigenmode solutions will involve some sort of average over the local real frequencies due to Doppler shift and diamagnetic drift. Although this real frequency is ultimately determined from boundary conditions, this dispersion relation should still be satisfied approximately for the solution with $\mathbf{k}_\perp = -i\nabla_\perp \delta B/\delta B$. In principle, the wave vector (k_x) can be determined from the dispersion relation and compared locally with the solution. We shall come back to this later when we interpret the results of the eigenmode equation.

Global Analysis

The background magnetic field, pressure, density, and flow velocity profiles are important for solving for

the global mirror modes, and we base our study upon a steady state configuration modeled after a typical pass through the magnetosheath and magnetopause [*Song et al.*, 1993; *Paschmann et al.*, 1993]. In Figure 1 we display typical steady state radial profiles for northward IMF. Although a true steady state configuration requires at least two dimensions in order to properly model the normal gradients in the plasma flow, the ram pressure due to the normal component of the bulk flow in the magnetosheath is typically much smaller than the plasma and magnetic pressures and thus does not appreciably affect the gradients that enter though the plasma pressure and magnetic field, and thus the essential MHD profiles do satisfy a steady state solution to first order in $\rho V_0^2/(P + B^2/2)$. On the other hand, the Doppler effects may be reasonably modeled by specifying a small normal velocity profile which is meant to be similar to what one would expect from a two-dimensional steady state configuration. The region of interest is characterized by two spatial scales: L_τ is the scale length of the unstable region corresponding to the distance over which $\tau_{MHD} < 0$ and corresponds roughly to the width of the magnetosheath ($\approx 2-5R_E$ [*Fairfield*, 1971]), and L_{MP}, which represents the gradient scale length of the magnetopause (roughly about 500 km). Another important parameter is the Mach number M_A, which we define to be the ratio V_0/v_{A0}, where v_{A0} is the Alfvén velocity at $\bar{x} = 0$. The profile of V_0 is chosen to decrease from the bow shock slowly to a value of zero at the magnetopause. The Alfvén velocity is determined from the background density and magnetic field. Typical values for magnetosheath magnetic field and density are roughly (40–80) nT and (10–40) cm^{-3}. A typical Alfvén velocity based upon these numbers is 275 km/s.

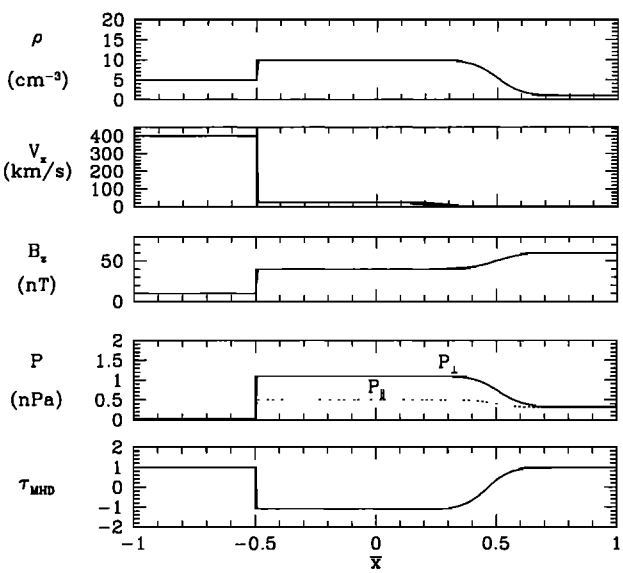

Figure 1. Model steady state profiles for the global mode analysis for $\Delta = L_{MP}/L_\tau = 0.05$ and $M_A = V_0/v_{A0} = 0.1$, where v_{A0} is the Alfvén velocity at $\bar{x} = 0$. L_{MP} and L_τ are the width of the magnetopause and magnetosheath, respectively.

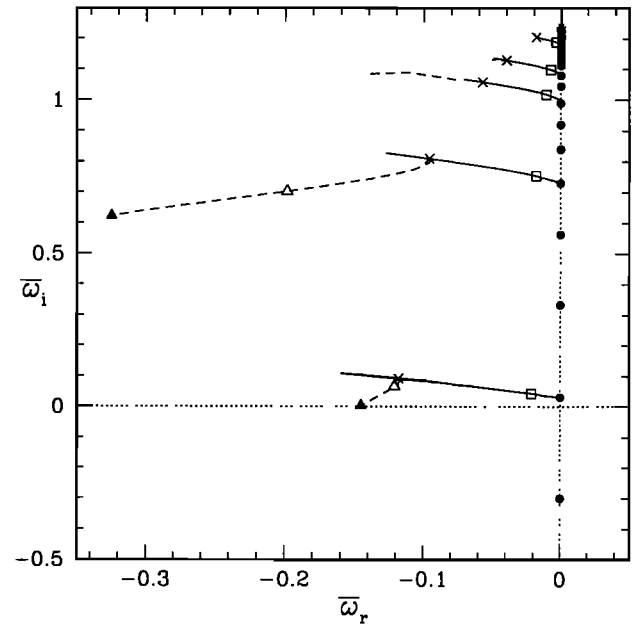

Figure 2. Evolution of the eigenfrequencies ($\bar{\omega} = \omega L_\tau/\pi v_{A0}$) of the eigenfunctions. The solid lines correspond to evolution of the roots in Δ with $M_A = 0$. The dashed lines correspond to evolution of the roots in M_A with $\Delta = 0.05$. Various points on these curves are indicated by symbols described in Table 1.

We solve (4) and (5) using (8)-(12) with these background profiles. The wave field is of the form $\delta B_\parallel = \delta B_\parallel(x)e^{i(k_y y + k_z z - \omega t)}$. The wave solutions are displayed in terms of the dimensionless radial coordinate, $\bar{x} = \pi x/L_\tau$, and dimensionless frequency, $\bar{\omega} = \omega L_\tau/\pi v_{A0}$. In these coordinates, the bow shock is at $\bar{x} = -0.5$ and magnetopause at $\bar{x} = 0.5$ and the width of the magnetosheath is therefore L_τ/π. The dimensionless frequency is chosen to be the fundamental frequency for standing Alfvén waves in the magnetosheath. The observed frequency would be $f = (10 - 100)\bar{\omega}$ mHz based upon typical values of L_τ and v_{A0} as given in the previous paragraph. The wave vectors in the directions perpendicular to x remain constant because of the one-dimensional nature of the equilibrium. These wave vectors are defined by k and θ where $k^2 = k_y^2 + k_z^2$ and $\theta = \tan^{-1}(k_y/k_z)$. The results displayed here have $k\pi/L_\tau = 5$ and $\theta = 30°$. For larger values of θ, the mode becomes more stable.

We want to investigate the importance of two effects on the eigenmode solutions. The first effect that we will study is that of gradients in the background magnetic field, temperature, and density at the magnetopause boundary. We shall vary the gradient scale at the magnetopause from a sharp boundary for which analytic solutions can be constructed to a realistic boundary where the gradient scale is approximately 10 ρ_i. The parameter that controls this effect is $\Delta = L_{MP}/L_\tau$ which will vary from 0 (sharp magnetopause) to 0.05 (realistic magnetopause). We expect that gradients will affect the

frequency and structure of the modes primarily through the kinetic effect due to diamagnetic drift frequency ω_*. The second effect that we shall consider is that of background flow $\mathbf{V}_0$. This effect will be controlled by the Alfvén Mach number M_A, which we shall vary from 0 to 0.2.

First, let us investigate the spectrum of eigenfrequencies for these modes. To illustrate the effects of background gradient (diamagnetic drift) and background plasma flow we plot in Figure 2 the evolution of the mode frequencies as functions of the magnetopause gradient scale and the plasma flow, $\mathbf{V}_0$. The large dots on the imaginary axis correspond to eigenfunctions with $\Delta = M_A = 0$ for which we can determine the eigenfrequency by solving a transcendental equation. The eigenfunctions corresponding to this spectrum of eigenfrequencies can be characterized by the number of nodes, n, in the radial wave function ($k_x \sim (n+1)\pi/L_\tau$). The nodes appear in ascending order starting from the damped fundamental and approach an accumulation point for large n. The accumulation point can be obtained as the root of $\tau(\omega) = 0$ evaluated in the region of instability. To study the effects of realistic Δ and M_A, we plot the evolution of the $n = 2, 5, 8, 10, 15$ modes. The solid curves show the evolution of the mode frequency as a function of $\Delta = L_{MP}/L_\tau$ with $\mathbf{V}_0 = 0$. The dashed curves show the evolution of modes as a function of M_A with $\Delta = 0.05$. Specific values of Δ and M_A are indicated by symbols described in Table 1.

Whereas for small L_{MP}, the modes all line up on the imaginary axis, as L_{MP} increases to more realistic values, the eigenvalues undergo excursions in the complex plane (illustrated by the solid curves of Figure 2) and are characterized by a significant real frequency. We interpret this real frequency to be the result of kinetic effects introduced by the diamganetic drift ω_*. The effective potential of (4) is inversely proportional to τ. Throughout most of the domain, $\tau_r \gg \tau_i$; however, near the magnetopause boundary τ_r passes through zero and contributions from τ_i become very important. If we inspect (14) for $\zeta \ll 1$ with $Z(\zeta) \sim i\sqrt{\pi}\zeta$ and $\omega_i \gg \omega_r$, we find that τ_i depends critically on diamagnetic drift effects and the real part of the eigenfrequency tries to balance ω_*. If ω_* were uniform the real frequency is identically ω_*, but for nonuniform diamagnetic effects, the real frequency arises as an averaged ω_*. As the scale of the magnetopause is increased, the real frequency increases. Note that although ω_* is only large near the magnetopause boundary, the frequency, which is a global property of the eigenmode, depends strongly on the profile at the boundary. In effect, information at the boundary is projected throughout the entire domain.

Table 1. Specific Values of Δ and M_A Indicated in Figure 2

Symbol	Δ	M_A
Solid circle	0	0
Open square	0.01	0
Cross	0.05	0
Open triangle	0.05	0.1
Solid triangle	0.05	0.2

The effects of plasma flow are also presented in the dashed curves in Figure 2. For substantial plasma flow ($M_A > 0.1$) the higher n modes are suppressed for $n > 8$. The lower n pick up a substantial real frequency contribution which we interpret as resulting from an averaged Doppler shift from the plasma frame to frame of the calculation. To understand the origin of the relatively larger real frequency, we note that the mode is most unstable when the argument of the Z functions $(\omega - \mathbf{k}\cdot\mathbf{V}_0)$ is small so that $\omega - \mathbf{k}\cdot\mathbf{V}_0 \simeq 0$ and the wave has a real frequency close to an average value of $\mathbf{k}\cdot\mathbf{V}_0$. We should point out, however, that there is substantial local deviation in this real frequency from the expected Doppler shift. Indeed, because the real frequency of the mode is fixed over the entire domain, the constancy of the locally defined $k_x V_0$ is a good measure of whether the real frequency is not observed in the plasma frame (at least in the regions where background gradients are small). However, it is a property of the solutions that k_x (defined in the WKB sense) oscillates about some average value, and hence locally there is significant deviation from the Doppler-shifted frequency (even up to a factor of 5 near the boundary). However, in an average sense, there seems to be a linear relationship between the real frequency and background flow V_0. (Note that we have not included the $\hat{y}$ component of flow which would lead to a further Doppler shift in the real frequency.)

We have shown the behavior of the eigenvalues and how the mode frequencies can differ significantly from the predictions of local theory when realistic gradients and plasma flow are introduced. Now let us turn our attention to the radial wave structure of the eigenmodes. In Figure 3 we illustrate three radial wave structures of the n=5 eigenmode for three different plasma flow velocity and magnetopause boundary layer thickness. The location $\bar{x} = -0.5$ corresponds to the bow shock position and $\bar{x} = 0.5$ the magnetopause position. The dotted and dashed lines correspond to the real and imaginary part of the eigenfunctions of $\delta B_\parallel$, respectively. In all of these three cases, the real frequency is negative (same sign as the ion diamagnetic drift frequency).

Because we choose a solution of the form $\delta B_\parallel = \delta B_\parallel(x) e^{i(k_y y + k_z z - \omega t)}$ the eigenmode equation becomes complex, and we solve a complex equation for the real and imaginary parts of $\delta B_\parallel$. The solution of the wave equation would be constructed from the real or imaginary part of $\delta B_\parallel = \delta B_\parallel(x) e^{i(k_y y + k_z z - \omega t)}$. What does this mean with regard to movement of wave structure? For negative real frequency, it is the case that if the real part of the eigenfunction leads the imaginary part,

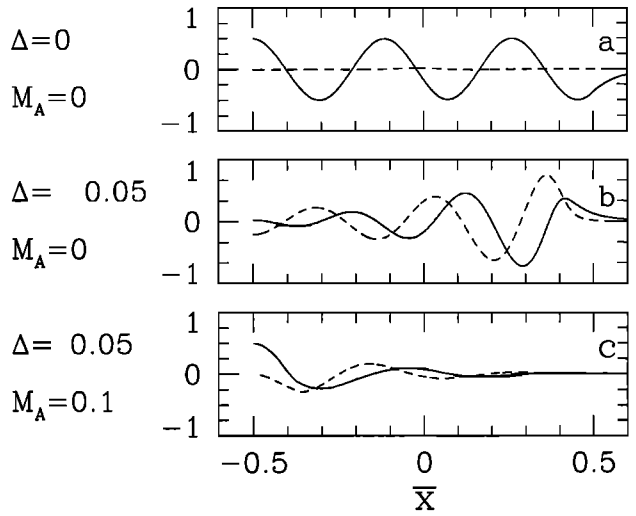

Figure 3. Three radial wave structures of $\delta B_{\|}$ (real: solid lines, imag: dashed lines) for the n=5 eigenmode for three different plasma flow velocity and magnetopause boundary layer thickness corresponding to three different points on the curve shown in Fig. 2. Notice that the density gradients and bulk flow strongly modify the mode structure. Note that n indicates the number of nodes of the eigenfunction.

then the mode structure travels to the left (phase velocity is negative). Conversely, if the imaginary part leads the real part, the wave structure travels to the right. This phase velocity is a phase velocity relative to the frame of the solution in which the bow shock and magnetopause are at a fixed location. If a satellite were to be stationed at some fixed point in the magnetosheath, it would observe wave structure to move past with the computed phase velocity (growing with the growth rate of the instability). We should also point out that the effective k_x is not constant.

In Figure 3a we plot the eigenfunction for a sharp magnetopause with zero layer width ($\Delta \to 0, V_0 = 0, \bar{\omega} = (0, 0.73)$. The eigenfunction is a standing structure which grows in time. The solution satisfies the local dispersion relation and has real wave vector. Note that the wave vector oscillates across the domain.

In Figure 3b we plot the $n = 5$ eigenfunction for a more realistic magnetopause gradient ($\Delta = 0.05, M_A = 0, \bar{\omega} = (-0.1, 0.81)$). In this case, the eigenfunction is complex and the real and imaginary parts of the eigenfunction are not in phase which is significant because $\bar{\omega}$ has a real part. Near the magnetopause where τ_{MHD} is small, the imaginary part of τ dominates over the real part and leads to a phase shift in the real and imaginary parts of the eigenfunction. Because there is a real frequency associated with the wave, the structure slowly propagates as it grows. The wave amplitude is largest near the magnetopause.

We can understand why the eigenmode is skewed by considering the local dispersion relation obtained from (13) and (14) in the magnetosheath region far away from the magnetopause boundary such that the local approximation is somewhat reasonable. The mode has largest growth with $k_{\|} > k_y$ and $\omega < k_{\|} V_A$ so that $\tau k_x^2 \approx -\sigma k_{\|}^2$ (essentially the same approximation used to obtain (18)). In the magnetosheath, background gradients are small, and therefore the drift terms in (14) can be neglected. Moreover, the eigenfrequency satisfies $|\omega/k_{\|} v_{th}| \ll 1$ and $\omega_r < \omega_i$. In this approximation, it is straightforward to see that $\tau_r \approx \tau_{MHD} < 0$ and $\tau_i \approx -\sqrt{\pi}(\beta_{\perp} T_{\perp}/T_{\|})\omega_r/k_{\|} v_{th}$ with $|\tau_r| \gg |\tau_i|$. The local wave vector should then satisfy $\tau k_x^2 \approx -\sigma k_{\|}^2$ which has the solution $k_x \approx \pm k_0(1 + i\delta)$, where $k_0 = |k_{\|}|\sqrt{-\sigma/\tau_r}$ and $\delta = -\tau_i/2\tau_r$. For $\omega_r < 0$, $\tau_i > 0$ and $\delta > 0$. By inspection of the eigenfunction, $k_{xr} < 0$ (the imaginary part of the eigenfunction leads the real part), and hence the eigenfunction has the spatial behavior, $\exp(-ik_0 x + \delta k_0 x)$, which increases in amplitude in the positive x direction. Because the real frequency is a consequence of the diamagnetic drift at the magnetopause, this growth can be interpreted to result from coupling of the wave with the diamagnetic drift associated with the pressure gradient. The diamagnetic drift causes the waves to drift with phase velocity toward the magnetopause boundary where the phase velocity slows and the wave amplitude is enhanced. Although the diamagnetic drift is only large near the magnetopause, its effects are globally transmitted throughout the entire spatial domain leading to a slowly propagating mirror mode with real frequency.

Finally, in Figure 3c we plot the eigenfunction when the plasma flow is included ($\Delta = 0.05, M_A = 0.1, \bar{\omega} = (-0.2, 0.7)$) the real frequency of the mode is some combination of an averaged $\mathbf{k} \cdot \mathbf{V}_0$ and ω_*. The real and imaginary parts of the eigenfunction are again out of phase with the imaginary part of the eigenfunction leading the real part of the eigenfunction so that the phase velocity is toward the magnetopause. However, the solutions are skewed toward the bow shock. The behavior of the amplitude can be understood from the dispersion relation resulting from (13) and (14). The arguments in the preceding paragraph apply equally well to this case with $\omega \to \omega - \mathbf{k} \cdot \mathbf{V}_0$ and the small frequency approximation $|(\omega - \mathbf{k} \cdot \mathbf{V}_0)/k_{\|} v_{th}| \ll 1$. As in the previous case, τ_r is dominated by $\tau_{MHD} < 0$, but $\tau_i \approx -\sqrt{\pi}(\beta_{\perp} T_{\perp}/T_{\|})(\omega_r - \mathbf{k} \cdot \mathbf{V}_0)/k_{\|} v_{th}$. Inspecting the solution, we find that the real part of the n=5 mode local wave vector varies in such a way that $\mathbf{k} \cdot \mathbf{V}_0/\omega_r \approx (2.5-5)$ throughout most of the domain and the sign of both ω and $\mathbf{k} \cdot \mathbf{V}_0$ is negative. This means that $\tau_i < 0$ which is opposite from the case without flow. As before, the local wave vector is $k_x \approx \pm k_0(1+i\delta)$ with $\delta = -\tau_i/2\tau_r < 0$ and $k_0 > 0$. By inspection of our solution, the real wave vector is dominantly negative, hence the mode has a spatial behavior, $\exp(-ik_0 x + \delta k_0 x)$ so that the mode decays with increasing values of x.

In review, we found that the solution has phase velocity directed toward the magnetopause, but the eigenmode has larger amplitude near the bow shock which

decreases in the direction of the magnetopause. In the frame of the moving plasma, the wave travels upstream against the flow and we found analytic solutions which predicted the spatial behavior of the amplitude. In order to better understand why wave energy is larger toward the bow shock, we checked the phase velocity which we obtain from the eigenfrequency and local wave vector, determined from the eigenmode solution and defined by ω_r/k_{xr}. We found that the phase velocity increases gradually from the bow shock toward the magnetopause. It is well known from geometrical optics that where a wave travels slowly its amplitude is larger and vice versa. Physically, the global mirror mode extracts energy from the unstable domain (where $\tau_{MHD} < 0$) in the magnetosheath. However, because the wave phase velocity is faster downstream than upstream, the wave carries more energy away from the downstream region than from the upstream region, or equivalently, the wave retains less energy in the downstream plasma region, and thus more wave energy remains upstream.

Discussion of Results

Our calculations support the idea that compressional waves observed in the magnetosheath are global mirror modes. First, we demonstrated that diamagnetic drift effects resulting from a realistic magnetopause profile produces a significant real frequency in the global mirror mode with an increase in amplitude near the magnetopause boundary. Moreover, there is a finite real phase velocity directed toward the magnetopause. The observations of *Song et al.* [1994] found the compressional wave phase velocity directed away from the magnetopause in the frame of the moving plasma, while the observations of *Gleaves and Southwood* [1991] seemed to indicate that compressional waves propagate toward the magnetopause. Second, when the plasma flow is introduced, the global mirror mode develops a phase velocity in the direction of the flow but is slower than the flow velocity. The result is that the wave would be observed to propagate toward the bow shock in the frame of the moving plasma and would have a finite real frequency in the plasma frame. The results also would seem to indicate that mirror mode wave activity should be stronger in the middle magnetosheath than near the magnetopause boundary which is consistent with observations by *Song et al.* [1994]. The essential result of this work is that finite real frequency is associated with the global mirror mode due to nonlocal effects and the wave has a finite phase velocity relative to the plasma flow.

In general, the actual wave structure at the magnetopause will consist of a large number of modes because the growth rates for the modes are approximately the same (see Figure 2). It is expected that finite Larmor radius effects will suppress the modes with sufficiently large k_x and that there will be some range of k_x with maximum growth. We expect that the observations will consist of many such modes with different k_x. As a result, there will be substantial beating between the waves leading to mirror mode wave structures with shorter spatial scale which would be comparable with the scales that are observed. The theory predicts a skew in the amplitude toward the magnetopause for small radial plasma flow and a skew toward the magnetosheath for large radial plasma flow. These results should of course be tempered by the understanding that nonlinear effects, perhaps to a significant degree, control the amplitudes of these waves. However, it is not unlikely that the general trend of the instability might be observed. These are predictions from the theory that can be compared with the observations in order to determine whether further refinements might be required for the theory.

The result of the one-dimensional hybrid simulation of *Omidi and Winske* [1995] differs from our analysis in a number of ways. Their analysis, for example, does not include the effect of diamagnetic drift because the wave vector $\mathbf{k}$ is only along $\nabla(P, B, n)$. Moreover, the background model that they use is not in steady state and therefore has time-dependent boundary conditions. It seems that the real frequency of the MIAOW waves results from the plasma flow effect because there is no diamagnetic drift effects in the simulation.

Our one-dimensional analysis can still be improved by including coupling between the compressional and transverse components of the perturbed magnetic field which becomes essential near the shear Alfvén and slow magnetosonic resonances. If the flow velocity is large and/or the diamagnetic drift is small, (4) contains a singularity where $\tau(x) = M_A^2$. For an isotropic plasma, this singularity occur at $M_A = 1$ and results because compressional waves cannot propagate against bulk flow which exceeds the Alfvén velocity. On the other hand, in anisotropic plasmas with no flow, the same singularity occurs where $\tau = 0$ which corresponds to the transition between a region unstable to mirror mode and a region stable to mirror mode such as at the plasma depletion layer. If the density and pressure gradients are sufficiently large, the singularity is resolved by diamagentic drift effects. Moreover, in anisotropic plasmas this singularity also corresponds to the slow magnetosonic resonance condition. Therefore it is likely that coupling to the sound wave will be important near that location. If the flow speed is sufficiently large, the resonance location will be shifted upstream. When the flow speed becomes too large no solution is found when $\tau = M_A^2$ because the diamagnetic effects no longer resolve the singularity. Resolution of the singularity involves coupling to the transverse magnetic field that we have neglected. In our future work we will include full coupling to the transverse magnetic field which resolves the singularity.

Summary

In this paper we have presented an eigenmode analysis of the global mirror mode at the magnetopause using

the kinetic-MHD model which accounts for both kinetic effects and global effects due to background gradients. The analysis demonstrates the following:

1. Magnetopause gradients and plasma flow lead to a substantial real part of the eigenfrequency for the global mirror modes which is of the order of a combination of the Doppler shift frequency associated with plasma flow and diamagnetic drift frequencies. However, the frequency differs significantly from the local Doppler shift associated with the eigenmode structure.

2. Pressure and density gradients at the magnetopause modify the wave structure because of diamagnetic drift effects. The real frequency associated with the diamagnetic drift frequency provides a wave phase velocity in the direction of the magnetopause. For small flow, the phase speed decreases toward the magnetopause and energy accumulates against the magnetopause boundary and the amplitude is skewed in that direction.

3. Bulk plasma flow also imparts a real phase velocity to the mode structure in the direction of the flow. However, this phase velocity is smaller than the flow velocity and the wave structure lags behind the flow. Moreover, the wave phase speed increases from the bow shock toward the magnetopause eventually approaching the flow velocity. As a result, the wave amplitude is large in the region where the phase velocity is small (near the bow shock) and is small where the phase velocity becomes large (toward the magnetopause), and thus the wave amplitude is skewed in the direction of the bow shock.

4. Boundary conditions are important because they impose restrictions that determine the global solution far away from the boundary and determine how the waves propagate within the region of instability.

5. The kinetic-MHD formalism is useful when it is important to consider both global scale gradients and kinetic effects.

One obvious direction for future consideration is an extension to obtain mirror mode solutions based on a two-dimensional magnetosheath-magnetopause configuration which includes the two-dimensional plasma flow and the effects of curvature. Another important area for further consideration is coupling between the compressional and transverse components of the perturbed magnetic field which becomes essential near the shear Alfvén and slow magnetosonic resonances. Because these modes have a real frequency, they can couple strongly with the kinetic Alfvén wave near the location where the real frequency matches the local shear Alfvén resonance frequency which will occur if the background magnetic field rotates. Such coupling could lead to enhanced particle transport across the magnetopause boundary layer.

Appendix: Integrals Over Products of Bessel Functions

In the kinetic-MHD equations, the wave fields are multiplied by J_0 and J_1 so that integrals over the product $J_0 J_1$ are frequently encountered. Integrals of this type may be evaluated through differentiation on the well-known integral 6.633.1 from *Gradshteyn and Ryzhik* [1963]:

$$\mathcal{I}_1(\alpha,\lambda) \equiv \int_0^\infty \exp(-\alpha\xi^2)[J_0(\lambda\xi)]^2\xi d\xi = \frac{1}{2\alpha}\exp(-\lambda^2/2\alpha)I_0(\lambda^2/2\alpha), \tag{A1}$$

where I_0 is the modified Bessel function.

Kinetic effects for the core plasma involve three integrals

$$\mathcal{I}_2 \equiv \int_0^\infty \exp(-\xi^2)J_0(\lambda\xi)J_1(\lambda\xi)\xi^2 d\xi \tag{A2}$$

$$\mathcal{I}_3 \equiv \int_0^\infty \exp(-\xi^2)J_0(\lambda\xi)J_1(\lambda\xi)\xi^4 d\xi \tag{A3}$$

$$\mathcal{I}_5 \equiv \int_0^\infty \exp(-\xi^2)J_0(\lambda\xi)J_1(\lambda\xi)\xi^6 d\xi. \tag{A4}$$

Using the relationship

$$\frac{\partial J_0(z)}{\partial z} = -J_1(z), \tag{A5}$$

we find that

$$\mathcal{I}_2 = -\frac{1}{2}\frac{\partial \mathcal{I}_1}{\partial \lambda}\bigg|_{\alpha=1} \tag{A6}$$

$$\mathcal{I}_3 = \frac{1}{2}\frac{\partial^2 \mathcal{I}_1}{\partial\lambda\partial\alpha}\bigg|_{\alpha=1} \tag{A7}$$

$$\mathcal{I}_5 = -\frac{1}{2}\frac{\partial^3 \mathcal{I}_1}{\partial\lambda\partial\alpha^2}\bigg|_{\alpha=1}. \tag{A8}$$

We find through differentiation using the rules

$$2\frac{\partial I_n(z)}{\partial z} = I_{n-1}(z) + I_{n+1}(z) \tag{A9}$$

$$\frac{2n}{z}I_n(z) = I_{n-1}(z) - I_{n+1}(z) \tag{A10}$$

with the auxiliary definition

$$\Gamma_n(z) = \exp(-z)I_n(z) \tag{A11}$$

that

$$\mathcal{I}_2 = \frac{\lambda}{4}[\Gamma_0 - \Gamma_1] \tag{A12}$$

$$\mathcal{I}_3 = \frac{\lambda}{2}\left\{[1-\lambda^2/2]\Gamma_0 - [1-\lambda^2]\Gamma_1/2\right\} \tag{A13}$$

$$\mathcal{I}_5 = \frac{3\lambda}{2}\left\{[1-11\lambda^2/12+\lambda^4/6]\Gamma_0 - [1-9\lambda^2/4+\lambda^4/2]\Gamma_1/3\right\} \tag{A14}$$

where the argument of Γ_n is $\lambda^2/2$.

The limiting forms of these expressions are of interest. The power series representations (in λ) of these functions is

$$\mathcal{I}_2 = \frac{\lambda}{4}(1 - 3\lambda^2/4 + 5\lambda^4/16 + \ldots \tag{A15}$$

$$\mathcal{I}_3 = \frac{\lambda}{2}(1 - 9\lambda^2/8 + 5\lambda^4/8 + ... \quad \text{(A16)}$$

$$\mathcal{I}_5 = \frac{3\lambda}{2}(1 - 3\lambda^2/2 + 25\lambda^4/24 + ... \quad \text{(A17)}$$

The asymptotic expansions for large λ are

$$\mathcal{I}_2 \sim \frac{1}{4\sqrt{\pi}\lambda^2} \quad \text{(A18)}$$

$$\mathcal{I}_3 \sim \frac{1}{8\sqrt{\pi}\lambda^2} \quad \text{(A19)}$$

$$\mathcal{I}_5 \sim \frac{3}{16\sqrt{\pi}\lambda^2} \quad \text{(A20)}$$

Acknowledgments. The authors would like to thank P. Song for useful discussions about magnetosheath wave observations. This work is supported by the NSF grant ATM-9523331 and the DoE contract DE-AC02-76-CHO3073.

The editor thanks B. J. Anderson and D. W. Swift for their assistance in evaluating this paper.

References

Anderson, B. J., S. A. Fuselier, and D. Murr, Electromagnetic ion cyclotron waves observed in the plasma depletion layer, *Geophys. Res. Lett.*, *18*, 1955–1958, 1991.

Anderson, B. J., S. A. Fuselier, S. P. Gary, and R. E. Denton, Magnetic spectral signatures in the Earth's magnetosheath and plasma depletion layer, *J. Geophys. Res.*, *99*, 5877–5891, 1994.

Chen, L., and A. Hasegawa, A theory of long-period magnetic pulsations, 1, steady state excitation of field line resonance, *J. Geophys. Res.*, *79*, 1024–1032, 1974.

Cheng, C. Z., A kinetic-magnetohydrodynamic model for low-frequency phenomena, *J. Geophys. Res.*, *96*, 21,159–21,171, 1991.

Cheng, C. Z., and J. R. Johnson, A kinetic-MHD model for low frequency multiscale phenomena, in *Physics of Space Plasmas (1995)*, MIT Center For Theoretical Geo/Cosmos Plasma Physics, Cambridge, Mass., pp. 127–145, 1996.

Denton, R. E., S. P. Gary, X. Li, B. J. Anderson, J. W. LaBelle, and M. Lessard, Low-frequency fluctuations in the magnetosheath near the magnetopause, *J. Geophys. Res.*, *100*, 5665–5679, 1995.

Fairfield, D. H., Average and unusual locations of the Earth's magnetopause and bow shock, *J. Geophys. Res.*, *76*, 6700–6716, 1971.

Frieman, E. A., and L. Chen, Nonlinear gyrokinetic equations for low-frequency electromagnetic waves in general plasma equilibria, *Phys. Fluids*, *25*, 502–508, 1982.

Gary, S. P., The mirror and ion-cyclotron instabilities, *J. Geophys. Res.*, *97*, 8519–8529, 1992.

Gary, S. P., and D. Winske, Simulations of ion cyclotron anisotropy instabilities in the terrestrial magnetosheath, *J. Geophys. Res.*, *98*, 9171–9179, 1993.

Gary, S. P., R. E. Denton, S. A. Fuselier, M. E. McKean, and D. Winske, Ion anisotropies in the magnetosheath, *Geophys. Res. Lett.*, *20*, 1767–1770, 1993a.

Gary, S. P., S. A. Fuselier, and B. J. Anderson, Ion anisotropy instabilities in the magnetosheath, *J. Geophys. Res.*, *98*, 1481–1488, 1993b.

Gary, S. P., M. E. McKean, and D. Winske, Ion cyclotron anisotropy instabilities in the magnetosheath: Theory and simulations, *J. Geophys. Res.*, *98*, 3963–3971, 1993c.

Gleaves, D. G., and D. J. Southwood, Magnetohydromagnetic fluctuations in the Earth's magnetosheath at 1500 LT: ISEE 1 and ISEE 2, *J. Geophys. Res.*, *96*, 129–142, 1991.

Gradshteyn, I. S., and I. M. Ryzhik, *Table of Integrals, Series and Products.* Academic, San Diego, Calif., 1963.

Hasegawa, A., Drift mirror instability in the magnetosphere, *Phys. Fluids*, *12*, 2642, 1969.

Hasegawa, A., and K. Mima, Anomalous transport produced by kinetic Alfvén wave turbulence, *Phys. Rev. Lett.*, *36*, 1362, 1978.

Hubert, D., C. C. Harvey, and C. T. Russell, Observations of magnetohydrodynamic modes in the Earth's magnetosheath, *J. Geophys. Res.*, *94*, 17305–17309, 1989.

Johnson, J. R., and C. Z. Cheng, Transport at the magnetopause—A kinetic-MHD description for a high-β plasma including finite Larmor radius effects, *Eos Trans. AGU*, *76*(17), 252, Spring Meet. Suppl., 1995.

Lee, L. C., J. R. Johnson, and Z. W. Ma, Kinetic Alfvén waves as a source of plasma transport at the dayside magnetopause, *J. Geophys. Res.*, *99*, 17405–17411, 1994.

Omidi, N., and D. Winske, Structure of the magnetopause inferred from one-dimensional hybrid simulations, *J. Geophys. Res.*, *100*, 11,935–11,955, 1995.

Paschmann, G., W. Baumjohann, N. Sckopke, and T. D. Phan, Structure of the dayside magnetopause for low magnetic shear, *J. Geophys. Res.*, *98*, 13,409–13,422, 1993.

Phan, T. D., et al., The subsolar magnetosheath and magnetopause for high solar wind ram pressure: WIND observations, *Geophys. Res. Lett.*, *23*, 1279–1282, 1996.

Song, P., C. T. Russell, R. J. Strangeway, J. R. Wygant, C. A. Cattell, R. J. Fitzenreiter, and R. R. Anderson, Wave properties near the subsolar magnetopause: Pc 3–4 energy coupling for northward interplanetary magnetic field, *J. Geophys. Res.*, *98*, 187–196, 1993.

Song, P., C. T. Russell, and S. P. Gary, Identification of low-frequency fluctuations in the terrestrial magnetosheath, *J. Geophys. Res.*, *99*, 6011–6025, 1994.

Southwood, D. J., and M. G. Kivelson, Mirror instability: 1. Physical mechanism of linear instability, *J. Geophys. Res.*, *98*, 9181–9187, 1993.

Tsurutani, B. T., E. J. Smith, R. R. Anderson, K. W. Ogilvie, J. D. Scudder, D. N. Baker, and S. J. Bame, Lion roars and nonoscillatory drift mirror waves in the magnetosheath, *J. Geophys. Res.*, *87*, 6060–6072, 1982.

C. Z. Cheng and Jay R. Johnson, Princeton Plasma Physics Laboratory, Princeton University Princeton, NJ 08543. (e-mail: jrj@pppl.gov)

(Received June 25, 1996; revised October 31, 1996; accepted December 17, 1996.)